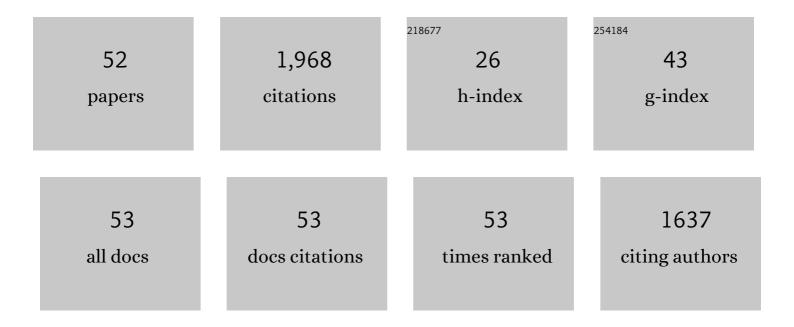
## Yashar Behnamian

List of Publications by Year in descending order

Source: https://exaly.com/author-pdf/5895509/publications.pdf Version: 2024-02-01



#	Article	IF	CITATIONS
1	A-site deficient perovskite: the parent for in situ exsolution of highly active, regenerable nano-particles as SOFC anodes. Journal of Materials Chemistry A, 2015, 3, 11048-11056.	10.3	164
2	Friction stir welding joint of dissimilar materials between AZ31B magnesium and 6061 aluminum alloys: Microstructure studies and mechanical characterizations. Materials Characterization, 2015, 101, 189-207.	4.4	153
3	A comparative study of oxide scales grown on stainless steel and nickel-based superalloys in ultra-high temperature supercritical water at 800 ŰC. Corrosion Science, 2016, 106, 188-207.	6.6	121
4	Development of electroless Ni–P/nano-WC composite coatings and investigation on its properties. Surface and Coatings Technology, 2015, 277, 99-106.	4.8	115
5	A mechanistic study on thiosulfate-enhanced passivity degradation of Alloy 800 in chloride solutions. Electrochimica Acta, 2013, 111, 510-525.	5.2	81
6	Review—Electrochemical Noise Applied in Corrosion Science: Theoretical and Mathematical Models towards Quantitative Analysis. Journal of the Electrochemical Society, 2020, 167, 081507.	2.9	78
7	Molybdenum doped Pr0.5Ba0.5MnO3â~`δ (Mo-PBMO) double perovskite as a potential solid oxide fuel cell anode material. Journal of Power Sources, 2016, 301, 237-241.	7.8	76
8	Electrochemical noise: a review of experimental setup, instrumentation and DC removal. Russian Journal of Electrochemistry, 2015, 51, 593-601.	0.9	73
9	Effect of solutionizing and aging on the microstructure and mechanical properties of powder bed binder jet printed nickel-based superalloy 625. Materials and Design, 2016, 111, 482-491.	7.0	69
10	Review-material degradation assessed by digital image processing: Fundamentals, progresses, and challenges. Journal of Materials Science and Technology, 2020, 53, 146-162.	10.7	54
11	Measuring atmospheric corrosion with electrochemical noise: A review of contemporary methods. Measurement: Journal of the International Measurement Confederation, 2019, 138, 54-79.	5.0	49
12	Monododecyl Phosphate Film on LY12 Aluminum Alloy: pH-Controlled Self-Assembly and Corrosion Resistance. Journal of the Electrochemical Society, 2020, 167, 161510.	2.9	49
13	Review of micro-scale and atomic-scale corrosion mechanisms of second phases in aluminum alloys. Transactions of Nonferrous Metals Society of China, 2021, 31, 3205-3227.	4.2	48
14	A comparative study on the oxidation of austenitic alloys 304 and 304-oxide dispersion strengthened steel in supercritical water at 650 ŰC. Journal of Supercritical Fluids, 2017, 119, 245-260.	3.2	43
15	Review—Factors Influencing Sulfur Induced Corrosion on the Secondary Side in Pressurized Water Reactors (PWRs). Journal of the Electrochemical Society, 2019, 166, C49-C64.	2.9	42
16	Metallurgical investigations and corrosion behavior of failed weld joint in AISI 1518 low carbon steel pipeline. Engineering Failure Analysis, 2015, 53, 78-96.	4.0	41
17	Sensing corrosion within an artificial defect in organic coating using SECM. Sensors and Actuators B: Chemical, 2019, 280, 235-242.	7.8	41
18	Corrosion behavior of alloy 316L stainless steel after exposure to supercritical water at 500 °C for 20,000 h. Journal of Supercritical Fluids, 2017, 127, 191-199.	3.2	40

YASHAR BEHNAMIAN

#	Article	IF	CITATIONS
19	pH Effect on Sulfur-Induced Passivity Degradation of Alloy 800 in Simulated Crevice Chemistries. Journal of the Electrochemical Society, 2014, 161, C201-C214.	2.9	38
20	Internal oxidation and crack susceptibility of alloy 310S stainless steel after long term exposure to supercritical water at 500ŰC. Journal of Supercritical Fluids, 2017, 120, 161-172.	3.2	34
21	Identifying defect levels in organic coatings with electrochemical noise (EN) measured in Single Cell (SC) mode. Progress in Organic Coatings, 2019, 126, 53-61.	3.9	33
22	Review—Electrochemical Probes and Sensors Designed for Time-Dependent Atmospheric Corrosion Monitoring: Fundamentals, Progress, and Challenges. Journal of the Electrochemical Society, 2020, 167, 037513.	2.9	33
23	Metal pitting corrosion characterized by scanning acoustic microscopy and binary image processing. Corrosion Science, 2020, 170, 108685.	6.6	33
24	Understanding the interaction of thiosulfate with Alloy 800 in aqueous chloride solutions using SECM. Journal of Electroanalytical Chemistry, 2015, 744, 77-84.	3.8	31
25	Characterization of oxide scales grown on alloy 310S stainless steel after long term exposure to supercritical water at 500 ŰC. Materials Characterization, 2016, 120, 273-284.	4.4	31
26	Semiconductivity conversion of Alloy 800 in sulphate, thiosulphate, and chloride solutions. Corrosion Science, 2014, 87, 265-277.	6.6	30
27	Tribological behavior of ZK60 magnesium matrix composite reinforced by hybrid MWCNTs/B4C prepared by stir casting method. Tribology International, 2022, 165, 107299.	5.9	27
28	Corrosion and biological behavior of nanostructured 316L stainless steel processed by severe plastic deformation. Surface and Interface Analysis, 2015, 47, 978-985.	1.8	24
29	A-site deficient La0.2Sr0.7TiO3â^î^ anode material for proton conducting ethane fuel cell to cogenerate ethylene and electricity. Journal of Power Sources, 2015, 298, 23-29.	7.8	23
30	Atmospheric corrosion assessed from corrosion images using fuzzy Kolmogorov–Sinai entropy. Corrosion Science, 2017, 120, 251-256.	6.6	23
31	Effects of Si, Mn on the corrosion behavior of ferritic–martensitic steels in supercritical water (SCW) environments. Corrosion Science, 2020, 166, 108432.	6.6	23
32	Semiconductivity Conversion of Passive Films on Alloy 800 in Chloride Solutions Containing Various Concentrations of Thiosulfate. Journal of the Electrochemical Society, 2015, 162, C482-C486.	2.9	21
33	Correlation between Passivity Breakdown and Composition of Passive Film Formed on Alloy 690ÂStudied by Sputtering XPS and FIB-HRTEM. Journal of the Electrochemical Society, 2019, 166, C332-C344.	2.9	21
34	Thermodynamics and molecular dynamics investigation of a possible new critical size for surface and inner cohesive energy of Al nanoparticles. Journal of Nanoparticle Research, 2011, 13, 6059-6067.	1.9	16
35	Passivation Degradation of Alloy 800 in Boiling Solution Containing Thiosulphate. Electrochimica Acta, 2017, 233, 13-25.	5.2	16
36	Anticorrosion performance of chromized coating prepared by pack cementation in simulated solution with H2S and CO2. Applied Surface Science, 2017, 419, 197-205.	6.1	16

YASHAR BEHNAMIAN

#	Article	IF	CITATIONS
37	Characterization of oxide layer and micro-crack initiation in alloy 316L stainless steel after 20,000 h exposure to supercritical water at 500 ŰC. Materials Characterization, 2017, 131, 532-543.	4.4	16
38	Reliability of the estimation of uniform corrosion rate of Q235B steel under simulated marine atmospheric conditions by electrochemical noise (EN) analyses. Measurement: Journal of the International Measurement Confederation, 2019, 148, 106946.	5.0	16
39	Pitting growth rate on Alloy 800 in chloride solutions containing thiosulphate: image analysis assessment. Corrosion Engineering Science and Technology, 2018, 53, 206-213.	1.4	14
40	An investigation into the dissolution characteristics of $\hat{I}^3$ precipitates in Mg-3Al-Zn alloy. Materials Research, 2014, 17, 996-1002.	1.3	13
41	A mechanistic study of sulfur-induced passivity degradation of Alloy 800 in a simulated alkaline crevice environment at 300 ŰC. Journal of Solid State Electrochemistry, 2015, 19, 3567-3578.	2.5	13
42	Effect of Tricalcium Magnesium Silicate Coating on the Electrochemical and Biological Behavior of Ti-6Al-4V Alloys. PLoS ONE, 2015, 10, e0138454.	2.5	12
43	Brief data overview of differently heat treated binder jet printed samples made from argon atomized alloy 625 powder. Data in Brief, 2016, 9, 556-562.	1.0	11
44	Electrochemical noise monitoring of the atmospheric corrosion of steels: identifying corrosion form using wavelet analysis. Corrosion Engineering Science and Technology, 0, , 1-9.	1.4	11
45	Alumina-Silica Composite Coatings on Aluminum by Plasma Electrolytic Oxidation: The Effect of Coating Time on Microstructure, Phase, and Corrosion Behavior. Journal of Materials Engineering and Performance, 2017, 26, 2663-2670.	2.5	9
46	Solution acidity and temperature induced anodic dissolution and degradation of through-plane electrical conductivity of Au/TiN coated metal bipolar plates used in PEMFC. Energy, 2022, 254, 124453.	8.8	8
47	Measuring the atmospheric corrosion of Q235B and T91 steels using gray value, wavelet analysis and fuzzy Kolmogorov–Sinai entropy. Anti-Corrosion Methods and Materials, 2019, 66, 621-630.	1.5	7
48	Pitting Corrosion Mechanism of Alloy 800 in Simulated Crevice Chemistries Containing Thiosulfate. Electrochemistry, 2016, 84, 585-596.	1.4	6
49	In-situ Study the Corrosion Degradation Mechanism of Tinplate in Salty Water by Scanning Electrochemical Microscopy. Russian Journal of Electrochemistry, 2018, 54, 216-223.	0.9	5
50	Effect of coating parameters on microstructure, corrosion behavior, hardness and formability of hot-dip Galfan and galvanized coatings. International Journal of Materials Research, 2021, 112, 321-332.	0.3	4
51	Memory effect and recoverability of passive film degradation of Alloy 800 in simulated crevice chemistry. Nuclear Engineering and Design, 2014, 280, 57-61.	1.7	3
52	Application of DOE method in evaluating for split tensile strength of slag-based boroaluminosilicate geopolymers reinforced with steel fibers. Journal of the Australian Ceramic Society, 2022, 58, 135-144.	1.9	3